DOI 10.5012/bkcs.2011.32.6.2051

Evaluation of Toxicity and Gene Expression Changes Triggered by Oxide Nanoparticles

Pooja Dua,[†,‡,a] Kiran N. Chaudhari,[§,a] Chang Han Lee,[†] Nitin K. Chaudhari,[§] Sun Woo Hong,[†] Jong-Sung Yu,[§,*] Soyoun Kim,[‡,*] and Dong-ki Lee[†,*]

[†]*Global Research Laboratory for RNAi Medicine, Department of Chemistry and BK21 School of Chemical Materials Science, Sungkyunkwan University, Suwon 440-746, Korea. [*]E-mail: dklee@skku.edu*
[‡]*Department of Biomedical Engineering, Dongguk University, Seoul 100-715, Korea. [*]E-mail: skim@dongguk.edu*
[§]*Department of Advanced Materials Chemistry, BK21 Research Team, Korea University, Chungnam 339-700, Korea [*]E-mail: jsyu212@korea.ac.kr*
Received January 10, 2011, Accepted April 25, 2011

Several studies have demonstrated that nanoparticles (NPs) have toxic effects on cultured cell lines, yet there are no clear data describing the overall molecular changes induced by NPs currently in use for human applications. In this study, the *in vitro* cytotoxicity of three oxide NPs of around 100 nm size, namely, mesoporous silica (MCM-41), iron oxide (Fe_2O_3-NPs), and zinc oxide (ZnO-NPs), was evaluated in the human embryonic kidney cell line HEK293. Cell viability assays demonstrated that 100 μg/mL MCM-41, 100 μg/mL Fe_2O_3, and 12.5 μg/mL ZnO exhibited 20% reductions in HEK293 cell viability in 24 hrs. DNA microarray analysis was performed on cells treated with these oxide NPs and further validated by real time PCR to understand cytotoxic changes occurring at the molecular level. Microarray analysis of NP-treated cells identified a number of up- and down-regulated genes that were found to be associated with inflammation, stress, and the cell death and defense response. At both the cellular and molecular levels, the toxicity was observed in the following order: ZnO-NPs > Fe_2O_3-NPs > MCM-41. In conclusion, our study provides important information regarding the toxicity of these three commonly used oxide NPs, which should be useful in future biomedical applications of these nanoparticles.

Key Words : MCM-41, Fe_2O_3 nanoparticle, ZnO nanoparticle, HEK293, Microarray

Introduction

Nanoparticles (NPs) have increased surface area to weight ratios relative to the same materials in the non-nano size range. In addition to unusual physical properties, NPs are also more chemically reactive than larger particles, which can be either advantageous or harmful depending on their end use. The nanotech boom started around a decade ago and since then the use of NPs in consumer goods and biomedical applications has dramatically increased. NPs are increasingly applied as drug delivery vehicles, biosensors, imaging contrast reagents, and therapeutic agents. However, it is surprising that even today the scientific and industrial community has no sufficiently clear data on the overall effects of these NPs on human health.

NPs are easily internalized into cells[1,2] and some NPs have even been shown to cross the blood brain barrier[3-5] where they alter biological processes and cause toxicity. Various *in vitro* and *in vivo* studies indicate that some NPs are associated with serious toxicity issues. The most commonly used *in vitro* toxicity tests focus on whether potentially toxic agents result in cell death. However, sublethal cellular changes may also exist that are not visible in such toxicity screens, but may significantly affect biological processes at the organismal level. Hence, it is important to identify overall cellular changes mediated by NP exposure. Identification of molecular signatures of toxicity at the genomic or proteomic levels provides comprehensive and reliable high throughput data. These data can then be used to compare, classify, and grade a NP on a scale of toxicity. In the present study we identified the molecular signatures of toxicity associated with commonly used oxide NPs. We evaluated and compared three NPs, mesoporous silica, iron oxide and zinc oxide (all around 100 nm in size), in terms of toxicity on HEK293 human embryonic kidney fibroblast cells using a cell death assay and DNA microarray analysis. HEK293 cells are well characterized cells, and their relevance as a model for toxicity assessment in humans is well established.[6,7]

Mesoporous silica, due to their large surface areas and easy permeability, has great potential as drug delivery vehicles and biosensors. One of the most commonly used mesoporous silica NPs, MCM-41, contains a hexagonal arrangement of adjustable pore channels. MCM-41 has been shown to exert concentration dependent toxicity on human T cell lymphoma and adenocarcinoma cells, but was not shown to elicit any toxicity or cell differentiation in mesenchymal stem cells.[8-10] Nevertheless, some of the data on MCM-41 cell-based screens were found to be misleading due to the interference of MCM-41 itself with the 2,5-diphenyltetrazolium salt (MTT) used to asses toxicity.[11,12] Iron oxide NPs

[a]These authors contributed equally to this work.

(Fe_2O_3 or Fe_3O_4) have been widely applied as magnetic drug targeting systems[13,14] and contrast agents in magnetic imaging. Cell-based cytotoxicity studies have shown that human mesothelioma cells are sensitive to Fe_2O_3-NPs exposure, but rodent 3T3 cells are non-responsive.[15] In addition, when compared to other metal oxides, naked Fe_2O_3-NPs were found to have no inhibitory effects on human hematopoietic progenitor cell growth[16] and did not induce any inflammatory response in human endothelial cells,[17] but caused marginal toxicity in lung epithelial cells.[18] In view of the present literature, it is difficult to determine whether MCM-41 and Fe_2O_3-NPs are free of associated toxicity, as most of the studies to date have not thoroughly investigated their effects on overall molecular changes occurring in cells.

ZnO-NPs are one of the main constituents of sunscreens due to their UV filtering properties and are also used in the surface coatings of paints, plastics, and textiles to provide antibacterial and antifungal protection. In contrast to mesoporous silica and iron oxide NPs, the use of ZnO-NPs is raising concern as they have been shown to cause significant DNA damage and oxidative stress in a wide range of cell lines tested.[19-21] Therefore, conducting a parallel analysis of cellular and molecular changes in cells exposed to biologically relevant concentrations of MCM-41 and Fe_2O_3 NPs in comparison to ZnO-NPs will provide a better understanding of their toxicity.

Materials and Methods

Cell Culture and Nanoparticle Characterization. HEK293 cells were grown in Dulbecco's Modified Eagle's Medium (DMEM, Invitrogen, Carlsbad, CA, USA) containing 10% fetal bovine serum (Invitrogen) and 1% penicillin and streptomycin. MCM-41 and Fe_2O_3-NPs were prepared as previously published[19-21] and characterized as described in Supplementary Material. Surface morphology and synthesized sample size were examined by scanning electron microscopy (SEM, LEO 1455VP, Hitachi S-4700) at an acceleration voltage of 25 kV. Microscopic features of the samples were observed with a transmission electron microscope (TEM, EM 912 Omega) operated at 120 kV. Total pore volumes were determined from the amount of gas adsorbed at a relative pressure of 0.99. Pore size distribution was derived from the adsorption branches by the Barrett-Joyner-Halenda (BJH) method. Commercially prepared ZnO nanopowder, ≥ 100 nm in size, was obtained from Sigma Aldrich (St. Louis, MO, USA, Cat no: 544906). All the NPs were suspended in phosphate-buffered saline (PBS), sonicated, and immediately applied to HEK293 cells to minimize agglomeration. To further confirm the state of aggregation, NP test concentrations were prepared in DMEM containing 10% FCS and incubated in culture dishes at 37°C under humidified conditions for 24 h. Samples were then charged on grids and TEM images were acquired.

WST-1 Cell Viability Assay. HEK293 cells were seeded in 96-well cell culture plates at a density of 6×10^3 cells per well and incubated with MCM-41, Fe_2O_3 and ZnO NPs at various concentrations in complete DMEM for 24, 48 and 72 h. For each concentration, six replicates were measured. Following incubation, 10 μL of premixed WST-1 reagent (TaKaRa, Bio Inc., Shiga, Japan) were added to each well and further incubated for 2 h. Color development was measured at 450 nm using an ELISA plate reader. All absorbance values were corrected against a blank, which was the same as the test wells except that it was devoid of cells. Percent cell viability was calculated considering the untreated control as 100% viable. The IC_{50} and IC_{20} values were calculated from dose response curves. Cytotoxic effect of nanoparticle-associated ions released in culture medium was also evaluated. Nanoparticles were resuspended in complete medium at indicated concentrations and were incubated for 24, 48 and 72 h, following which the NP suspensions were centrifuged at 13,000 rpm for 10 min and the supernatant medium was collected. HEK293 cells were exposed to the so obtained conditioned medium for various time-points *viz* 24 h in presence of 24 h NP-supernatent, 48h in presence of 48 h NP-supernatent, 72 h in presence of 72 h NP-supernatent .

DNA Microarray. Cells were grown to 60% cell density and treated with 100 μg/mL MCM-41, 100 μg/mL Fe_2O_3, and 12.5 μg/mL ZnO in complete media for 24 h. Total RNA was extracted using the TRI Reagent® kit (Ambion, Austin, TX, USA) according to manufacturer's instructions. Total RNA (10 μg) was used for double-stranded cDNA (dscDNA) synthesis using a commercial kit (Invitrogen). Reactions were stopped with EDTA, treated with RNase A, and the dscDNA was ethanol-precipitated. One μg of dscDNA was used for labeling by Klenow fragments (New England Biolabs, Beverly, MA, USA) using a Cy3-labeled random 9mer (TriLink Biotechnologies, San Diego, CA, USA), and labeled samples were precipitated using isopropanol. Four μg of Cy3-labeled DNA (containing sample tracking control and alignment oligo) was hybridized to a NimbleGen 385K 4-plex human microarray for 18 h at 42 °C using the NimbleGen Hybridization system (Roche NimbleGen Inc., Madison, WI, USA). Arrays were washed and images were obtained using an InnoScan® 900 scanner (Innopsys, Carbonne, France). Scanned images were imported into Mapix software (Innopsys).

Microarray Data Analysis. Scanned images were imported into NimbleScan software. Expression data were normalized through quantile normalization and the Robust Multichip Average (RMA) algorithm.[22] MA plots were generated in which the X-axis represents the average $\log_2$ expression of the control and test samples and the Y-axis corresponds to the ratio of $\log_2$ expression value of the test to the control to visualize overall changes in gene expression. Fold change in expression for 24,000 genes was calculated for each NP relative to the non-treatment control. Transcripts with more than a 2-fold change in either direction were selected. Genes that were differentially expressed by the test materials were functionally categorized using a web-based program, Database for Annotation, Visualization and Integrated Discovery (DAVID) (http://david.abcc.ncifcrf.gov).[23]

Enrichment in gene ontology terms, for both up- and down-regulated genes, was determined by Fisher exact $p < 0.05$ and Count Threshold 2.

Quantitative Real-time PCR. RNA was extracted as described and 500 ng was used as a template for cDNA synthesis, using the High Capacity cDNA Reverse Transcription kit (Applied Biosystems) according to the manufacturer's protocol. Aliquots of the cDNA reaction mixture were analyzed by quantitative real-time PCR using a StepOne real-time PCR thermocycler (Applied Biosystems). Primers used for target specific amplification are shown in Table S2. All primer pairs spanned an intron to avoid possible genomic DNA contamination. The PCR amplification cycle involved denaturation at 95 ºC for 15s, annealing at 60 ºC for 20s, and extension at 72 ºC for 15s. Quantitative real time PCR data for each gene product were normalized by GAPDH transcript levels and are reported as the mean ± SE of relative change compared to the untreated control.

Results and Discussion

Particle Characterization. The MCM-41 particles were spherical in shape and approximately 110 nm in diameter, as shown in SEM and TEM images (Fig. S1). Each particle possessed mesoporous channels running throughout the particle with a pore size of 2.6 nm as indicated by the pore size distribution curve (Fig. S2). The Fe_2O_3 NPs synthesized in this work were demonstrated as hematite α-Fe_2O_3 by XRD pattern as previously published.[21] The SEM image in Figure S1 clearly reveals that the product was composed of a large quantity of uniform hexagonal prism-like α-Fe_2O_3. It was observed from the SEM and TEM images that the Fe_2O_3 sample exhibited a mainly hexagonal nanoplate form with an average parallel side, diagonal side, width, and thickness of 90-100 nm, 60-70 nm, 120-150 nm, and 85-95 nm, respectively. Commercially obtained ZnO nanopowder was ≥ 100 nm in size and had a surface area of 15-25 m^2/g. TEM images of NPs incubated in culture medium for 24 h suggest that no particle agglomeration was observed at 100 μg/mL of MCM-41 and Fe_2O_3 and at 12.5μg/mL ZnO (Figure S3).

Nanoparticle Cytotoxicity on HEK293 Cells. HEK293 cells were exposed to increasing concentrations of test NP materials for 24, 48 and 72 h and cell viability was then measured. All three NPs were earlier shown to be readily internalized into cultured mammalian cells.[8,17] The WST-1 assay is the most sensitive assay available to measure the metabolic activities of viable cells and has the least background interference. Moreover, unlike MTT, WST-1 assay results are not affected by MCM-41-mediated changes in cellular trafficking.[11] Dose response curves clearly show concentration dependent toxicity at all time points (Figure 1). Exposure duration did not significantly affect cell viability at lower MCM-41 and ZnO concentrations; however, at concentrations higher than the IC_{50} the extent of cytotoxicity seemed to correlate with the duration of exposure. IC_{50} values suggest that MCM-41 and Fe_2O_3 had very similar toxicity profiles for 24 and 48 h of incubation. Unlike MCM-41 and Fe_2O_3, ZnO-NPs showed a remarkably steep relationship between ZnO concentration and cell death at concentrations ranging between 15-20 μg/mL, leading to much higher IC_{50} values. A similar concentration dependent

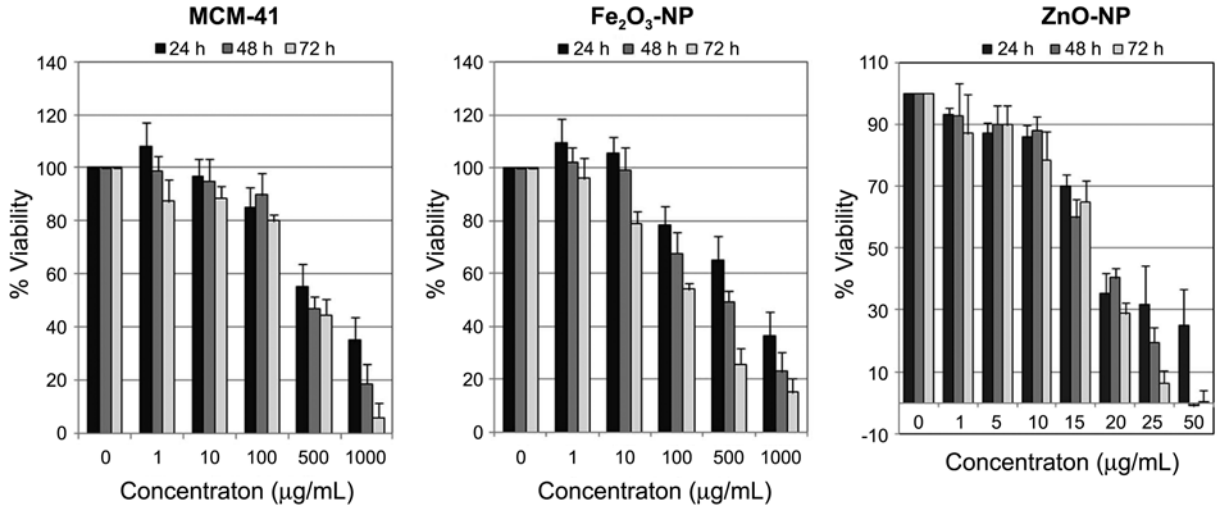

Duration of incubation	MCM-41 (μg/mL)	Fe_2O_3-NP (μg/mL)	ZnO-NP (μg/mL)
24 h	574	698	21.47
48 h	461	464	20.19
72 h	423	116	16.58

Figure 1. Effects of MCM-41, Fe_2O_3-NP, and ZnO-NP on HEK293 cell viability. Cell viability after 24, 48 and 72 h exposure to the test compounds was determined by WST-1 assays. The data are represented as the mean ± SE of three independent experiments and is expressed as percent cell viability with respect to the untreated control as 100% viable. The IC_{50} values of these NPs are given in Table below.

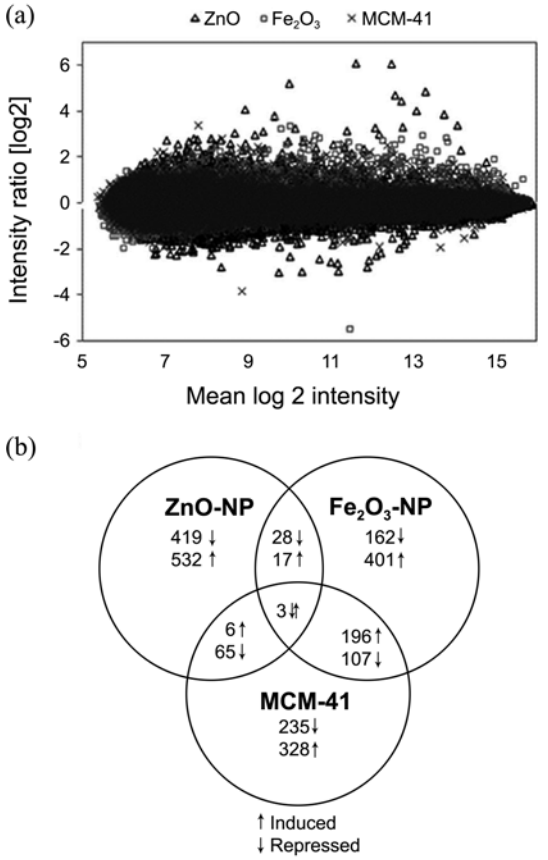

Figure 2. (a) MA Scatter plot showing overall distribution of gene expression upon NP exposure. (b) Venn diagrams illustrating genes induced or repressed by more than 2-fold upon nanoparticle exposure.

response towards ZnO-NPs with a sudden drop in cell viability has been reported in the literature.[19,24] Since metal oxide nanoparticles may be ionized during the sample preparation procedure and the subsequent ion leakage may result in a continuous formation of free radicals and metal ions,[25,26] we also assessed the toxicity imparted due to nanoparticle associated ions. HEK293 cells incubated with NP-conditioned medium suggest that at higher concentrations all the three oxide-NPs resulted in toxicity due to the ions released in the culture medium (Figure S4). Although the contribution of metal ion associated toxicity in MCM41 and Fe_2O_3 seems to fairly low, exposure to ZnO conditioned medium for longer duration resulted in substantial toxicity. Nonetheless, NPs showed much higher cytotoxicity than ions released from NPs for all NPs tested. For further comparative assessment of these NPs, the cell viability assay data was considered as a basis for choosing their equipotent concentrations. Moreover, to make the study more relevant, concentrations were selected that resembled doses at which these NPs are used for human applications. An IC_{20} (concentrations that lead to 20% loss in viability) value for 24 h incubation was considered, as in all three cases, MCM-41 (100 μg/mL)[27,28] Fe_2O_3 (100 μg/mL)[29,30] and ZnO (12.5 μg/mL)[31,32] the concentrations chosen were within the range used for biomedical or other applications.

Nanoparticle Mediated Gene Expression Changes in HEK293 Cells. We performed DNA microarray analysis of HEK293 cells exposed to IC_{20} concentrations of the selected NPs for 24 h to identify the molecular toxicity signature of the oxide NPs under study. The MA plots in Figure 2(a) (average intensity *vs.* intensity ratio) show the overall distributions of gene expression. The number of transcripts that had more than a 2-fold alteration in gene expression in either direction is shown in the Venn diagram (Figure 2(b)). As can be seen, the number and magnitude of genes that were induced were greater in number than those that were repressed. Even at similar cytotoxic concentrations, ZnO-NPs induced greater alterations in gene expression (both number and magnitude) in comparison to the other two test materials. Genes with altered expression and associations with cellular toxicity are listed in Table S1. The genes with altered expression were functionally annotated and the gene ontology (GO) terms with their respective fold-enrichment values were determined (Figure 3(a) and (b)).

Both Fe_2O_3 and MCM-41 induced expressions of many genes that encode for 40S and 60S ribosomal protein homologs. These two NPs also resulted in increased expression of various genes that encode for histones (histone 1, h2ad, h2a, h3 family b) involved in chromatin remodeling. CCL15, a cytokine involved in inflammation and chemotaxis[33] was up-regulated by both MCM-41 and Fe_2O_3. Further gene ontology analysis clearly showed that Fe_2O_3 induced more significant changes than MCM-41. Three genes that are associated with the JNK signaling pathway were up regulated upon Fe_2O_3 exposure (Table S1). JNK signaling is mainly involved in the maintenance of cell viability and proliferation in response to environmental fluctuations and stress.[34] In addition, genes involved in renal system processes, neuron development, and cell proliferation (natriuretic peptide precursor b, endothelin1 and 2, bone morphogenic protein, fibroblast growth factor 8) were also down regulated by Fe_2O_3 but not by MCM-41. Defense response and stress associated genes pregnancy specific beta1 glycoproteins (PSG1 and PSG2)[35] were significantly induced by Fe_2O_3 while only PSG1 was induced by MCM-41.

Unlike MCM-41 and Fe_2O_3 NPs, ZnO-NP resulted in the altered expression of many genes involved in cell death and apoptosis, indicating that even at low concentrations ZnO generates significant toxic responses in the cell. The induced genes included tumor necrosis factor ligands and receptors, interleukin1 beta, interleukin24, von hippel-lindau, somatostatin receptor2, phosphodiesterase7, matrix metalloprotease-9, growth arrest and DNA damage inducible alpha and gamma oncostatin m, protein kinase C gamma, fas apoptotic inhibitory molecule 3, inhibin beta a, and bcl2 like protein. In addition, many genes of the metallothionein family namely MT2a, MT1X, MT1g, MT1b, MT1f showed more than 10-fold induction upon ZnO-NP exposure. Metallothioneins are a family of cysteine rich metal binding proteins that are involved in metal detoxification and in the protection of cells against reactive oxygen species (ROS). In an earlier study,

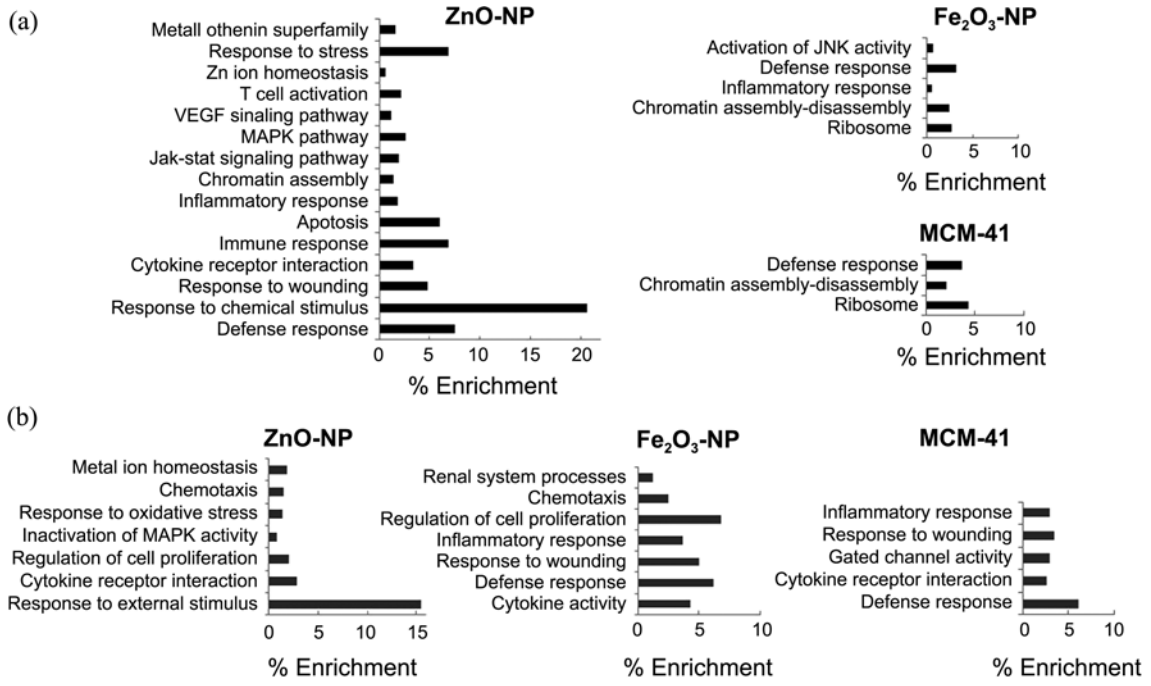

Figure 3. Categorization of greater than 2-fold altered genes on the basis of their gene ontology. (a) up-regulated (b) and down-regulated. Each bar represents the percent enrichment of the GO term against total altered genes as background.

silver NPs were shown to induce the expression of metallothionein genes in liver cells.[36] Most of the studies conducted with ZnO-NPs suggest that ZnO-mediated toxicity is primarily a result of oxidative stress and the generation of ROS.[19] In our study, in addition to the up-regulation of metallothioneins, we also observed reductions in eosinophil peroxidase and superoxide dismutase 2 mitochondrial (MnSOD) levels. Superoxide dismutase converts superoxide anion to hydrogen peroxide. In renal diseases, polycystic kidney damage oxidative stress and synthesis of H_2O_2 results in reduced mRNA levels of important antioxidant enzymes including MnSOD.[37] Reduction of mitochondrial SOD in our study suggests that upon prolonged exposure to ZnO NPs, the antioxidant activities of cells were compromised, which would further potentiate its toxicity. The findings of our study are also in agreement with earlier reports on ZnO-NPs in which similar changes in SOD expression and eosinophil peroxide transcription were observed.[17,19] We also observed induction of genes involved in Ca^{2+} homeostasis, namely protein kinase C gamma, S100 calcium binding protein, calbindin2, to name a few (Table S1). Some signaling pathways were also up regulated in ZnO-NPs treated samples, namely MAPK, Jak-Stat and VEGF signaling pathways.

Real Time PCR Validation of Key Toxicity Associated Genes. Based on the microarray expression changes and Gene Ontology search, eight genes that were up-regulated and associated with cellular toxicity were validated by real-time PCR. Among these, four genes, heat shock protein 6 (HSPA6), matrix metalloprotease 1 (MMP1), and pregnancy specific beta1 glycoprotein (PSG1, PSG9), showed more than 1.5-fold induction by all three NPs in the microarray analysis. Of the remaining four genes, chemokine C-C motif receptor 15 (CCL15) showed Fe_2O_3 and MCM-41 specific up-regulation, while v-fos fbj murine osteosarcoma viral oncogene homolog (vFOS fbj) was strongly induced by ZnO and to a lesser extent by Fe_2O_3. The interleukin17f (IL17f) and metallothionein 2a genes were specifically induced by ZnO. The fold changes in expressions of these genes obtained from microarray analysis are provided in Table S1. For all genes tested, the general dose response trends observed with real time PCR were consistent with microarray analyses (Fig. 4). However, in some cases the magnitude of fold induction seen in real-time PCR was higher than measured by microarray analysis, which was expected, as the dynamic range afforded by microarray is comparatively much lower. Only in the case of HSPA6 did we find that the microarray results were much higher than the actual changes in gene expression. Altogether, the results of real time PCR validation were in agreement with the microarray data, suggesting that the all three test materials induced expression of toxicity-associated genes. However, in comparison to Fe_2O_3 and MCM-41, ZnO exposure showed greater changes in expression, both in number and magnitude.

In conclusion, the data clearly show that although these three oxide NPs cause toxicity in cells, ZnO-NPs-mediated toxicity is much higher than those of MCM-41 and Fe_2O_3. Levels of cytotoxic response were observed in the following order: MCM-41 < Fe_2O_3-NPs < ZnO-NP. Gene ontology enrichment suggests that MCM-41 and Fe_2O_3 exposure, even at the concentrations used for various biomedical applications lead to toxic phenotypes in cells which can be classified as early response of cells towards environmental stressor. Although MCM-41 appeared to have marginal toxi-

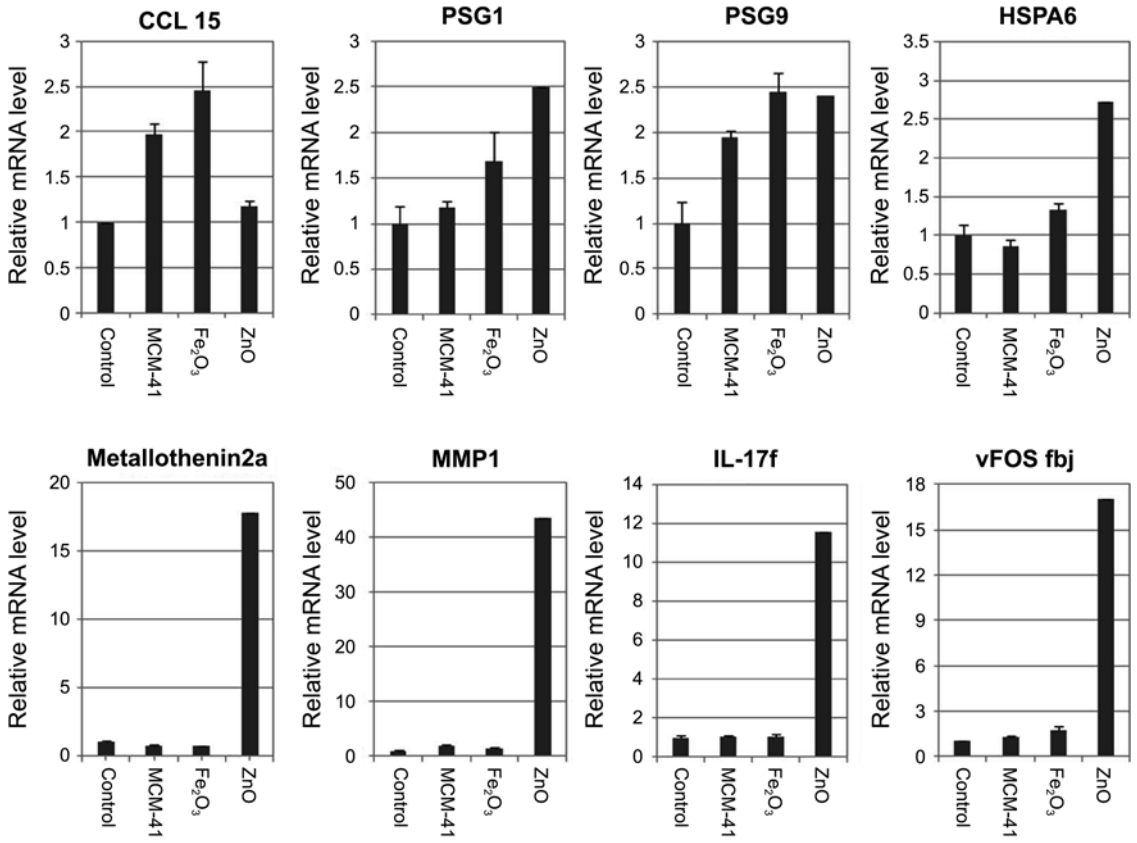

Figure 4. Real time PCR validation of selected genes that were found to be induced by NP exposure and have associations with toxic responses in the cells.

city, Fe_2O_3-NP-mediated alteration in gene expression implies toxicity above threshold levels, which the cell may or may not overcome depending upon the duration of exposure and the cell type. ZnO, even at lower concentrations, can induce substantial toxic responses in cells that are sufficient to trigger programmed cell death; hence, the use of ZnO for human applications should be scrutinized to establish safe levels prior to use. Therefore, our study shows that these NPs are more biologically challenging than originally thought. Further studies are needed to understand shape/size dependent cellular effects and the effects of surface modifications in overcoming these toxicity issues in order to provide a safe window for their end use.

Acknowledgments. This work was supported by a grant from the Ministry of Environment Eco-Technopia 21 Project (091-081-073) to D.-k. Lee. P.D. acknowledges support from the Sungkyunkwan University Post-Doctoral Fellowship in 2008.

References

1. Rothen-Rutishauser, B. M.; Schurch, S.; Haenni, B.; Kapp, N.; Gehr, P. *Environ. Sci. Technol.* **2006**, *40*, 4353-4359.
2. Huang, X.; Teng, X.; Chen, D.; Tang, F.; He, J. *Biomaterials* **2010**, *31*, 438-448.
3. Tang, J.; Xiong, L.; Wang, S.; Wang, J.; Liu, L.; Li, J.; Yuan, F.; Xi, T. *J. Nanosci. Nanotechnol.* **2009**, *9*, 4924-4932.
4. Oberdorster, G.; Elder, A.; Rinderknecht, A. *J. Nanosci. Nanotechnol.* **2009**, *9*, 4996-5007.
5. Long, T. C.; Saleh, N.; Tilton, R. D.; Lowry, G. V.; Veronesi, B. *Environ. Sci. Technol.* **2006**, *40*, 4346-4352.
6. Ji, L. L.; Chen, Y.; Wang, Z. T. *Exp. Toxicol. Pathol.* **2008**, *60*, 87-93.
7. Florea, A. M.; Splettstoesser, F.; Busselberg, D. *Toxicol. Appl. Pharmacol.* **2007**, *220*, 292-301.
8. Tao, Z.; Toms, B. B.; Goodisman, J.; Asefa, T. *Chem. Res. Toxicol.* **2009**, *22*, 1869-1880.
9. Di Pasqua, A. J.; Sharma, K. K.; Shi, Y. L.; Toms, B. B.; Ouellette, W.; Dabrowiak, J. C.; Asefa, T. *J. Inorg. Biochem.* **2008**, *102*, 1416-1423.
10. Huang, D. M.; Chung, T. H.; Hung, Y.; Lu, F.; Wu, S. H.; Mou, C. Y.; Yao, M.; Chen, Y. C. *Toxicol. Appl. Pharmacol.* **2008**, *231*, 208-215.
11. Fisichella, M.; Dabboue, H.; Bhattacharyya, S.; Saboungi, M. L.; Salvetat, J. P.; Hevor, T.; Guerin, M. *Toxicol. In Vitro* **2009**, *23*, 697-703.
12. Laaksonen, T.; Santos, H.; Vihola, H.; Salonen, J.; Riikonen, J.; Heikkila, T.; Peltonen, L.; Kumar, N.; Murzin, D. Y.; Lehto, V. P.; Hirvonen, J. *Chem. Res. Toxicol.* **2007**, *20*, 1913-1918.
13. Alexiou, C.; Jurgons, R.; Schmid, R.; Erhardt, W.; Parak, F.; Bergemann, C.; Iro, H. *Hno.* **2005**, *53*, 618-622.
14. Berry, C. C.; Wells, S.; Charles, S.; Curtis, A. S. *Biomaterials* **2003**, *24*, 4551-4557.
15. Brunner, T. J.; Wick, P.; Manser, P.; Spohn, P.; Grass, R. N.; Limbach, L. K.; Bruinink, A.; Stark, W. J. *Environ. Sci. Technol.* **2006**, *40*, 4374-4381.
16. Bregoli, L.; Chiarini, F.; Gambarelli, A.; Sighinolfi, G.; Gatti, A. M.; Santi, P.; Martelli, A. M.; Cocco, L. *Toxicology* **2009**, *262*, 121-129.

17. Kennedy, I. M.; Wilson, D.; Barakat, A. I. *Res. Rep. Health Eff. Inst.* **2009**, 3-32.
18. Karlsson, H. L.; Cronholm, P.; Gustafsson, J.; Moller, L. *Chem. Res. Toxicol.* **2008**, *21*, 1726-1732.
19. Huang, C. C.; Aronstam, R. S.; Chen, D. R.; Huang, Y. W. *Toxicol. In Vitro* **2009**.
20. Deng, X.; Luan, Q.; Chen, W.; Wang, Y.; Wu, M.; Zhang, H.; Jiao, Z. *Nanotechnology* **2009**, *20*, 115101.
21. Sharma, V.; Shukla, R. K.; Saxena, N.; Parmar, D.; Das, M.; Dhawan, A. *Toxicol. Lett* **2009**, *185*, 211-218.
22. Hong, S. W.; Hong, S. M.; Yoo, J. W.; Lee, Y. C.; Kim, S.; Lis, J. T.; Lee, D. K. *Proc. Natl. Acad Sci. USA* **2009**, *106*, 14276-14280.
23. Dennis, G., Jr.; Sherman, B. T.; Hosack, D. A.; Yang, J.; Gao, W.; Lane, H. C.; Lempicki, R. A. *Genome. Biol.* **2003**, *4*, P3.
24. Gojova, A.; Guo, B.; Kota, R. S.; Rutledge, J. C.; Kennedy, I. M.; Barakat, A. I. *Environ. Health Perspect.* **2007**, *115*, 403-409.
25. Cho, W. S.; Duffin, R.; Poland, C. A.; Duschl, A.; Oostingh, G. J.; Macnee, W.; Bradley, M.; Megson, I. L.; Donaldson, K. *Nanotoxicology* **2011**.
26. Baek, Y. W.; An, Y. J. *Sci. Total Environ.* **2011**, *409*, 1603-1608.
27. Radu, D. R.; Lai, C. Y.; Jeftinija, K.; Rowe, E. W.; Jeftinija, S.; Lin, V. S. *J. Am. Chem. Soc.* **2004**, *126*, 13216-13217.
28. Slowing, II.; Vivero-Escoto, J. L.; Wu, C. W.; Lin, V. S. *Adv. Drug. Deliv. Rev.* **2008**, *60*, 1278-1288.
29. Smirnov, P.; Lavergne, E.; Gazeau, F.; Lewin, M.; Boissonnas, A.; Doan, B. T.; Gillet, B.; Combadiere, C.; Combadiere, B.; Clement, O. *Magn. Reson. Med.* **2006**, *56*, 498-508.
30. Smirnov, P.; Gazeau, F.; Lewin, M.; Bacri, J. C.; Siauve, N.; Vayssettes, C.; Cuenod, C. A.; Clement, O. *Magn. Reson. Med.* **2004**, *52*, 73-79.
31. Cross, S. E.; Innes, B.; Roberts, M. S.; Tsuzuki, T.; Robertson, T. A.; McCormick, P. *Skin Pharmacol. Physiol.* **2007**, *20*, 148-154.
32. Nohynek, G. J.; Lademann, J.; Ribaud, C.; Roberts, M. S. *Crit. Rev. Toxicol.* **2007**, *37*, 251-277.
33. Pardigol, A.; Forssmann, U.; Zucht, H. D.; Loetscher, P.; Schulz-Knappe, P.; Baggiolini, M.; Forssmann, W. G.; Magert, H. J. *Proc. Natl. Acad Sci. U S A* **1998**, *95*, 6308-6313.
34. Nishina, H. W. T.; Katada, T. *J. Biochem.* **2004**, *136*, 123-126.
35. Snyder, S. K.; Wessner, D. H.; Wessells, J. L.; Waterhouse, R. M.; Wahl, L. M.; Zimmermann, W.; Dveksler, G. S. *Am. J. Reprod. Immunol.* **2001**, *45*, 205-216.
36. Kawata, K.; Osawa, M.; Okabe, S. *Environ. Sci. Technol.* **2009**, *43*, 6046-6051.
37. Maser, R. L.; Vassmer, D.; Magenheimer, B. S.; Calvet, J. P. *J. Am. Soc. Nephrol.* **2002**, *13*, 991-999.

DOI 10.5012/bkcs.2011.32.6.

Supporting Information

Evaluation of Toxicity and Gene Expression Changes Triggered by Oxide Nanoparticles

Pooja Dua,[†,‡,a] Kiran N. Chaudhari,[§,a] Chang Han Lee,[†] Nitin K. Chaudhari,[§] Sun Woo Hong,[†] Jong-Sung Yu,[§,*] Soyoun Kim,[‡,*] and Dong-ki Lee[†,*]

[†]*Global Research Laboratory for RNAi Medicine, Department of Chemistry and BK21 School of Chemical Materials Science, Sungkyunkwan University, Suwon 440-746, Korea. [*]E-mail: dklee@skku.edu (D.-k. Lee)*
[‡]*Department of Biomedical Engineering, Dongguk University, Seoul 100-715, Korea. [*]E-mail: skim@dongguk.edu (S. Kim)*
[§]*Department of Advanced Materials Chemistry, BK21 Research Team, Korea University, Chungnam 339-700, Korea*
[*]*E-mail: jsyu212@korea.ac.kr (J.S. Yu)*
Received January 10, 2011, Accepted April 25, 2011

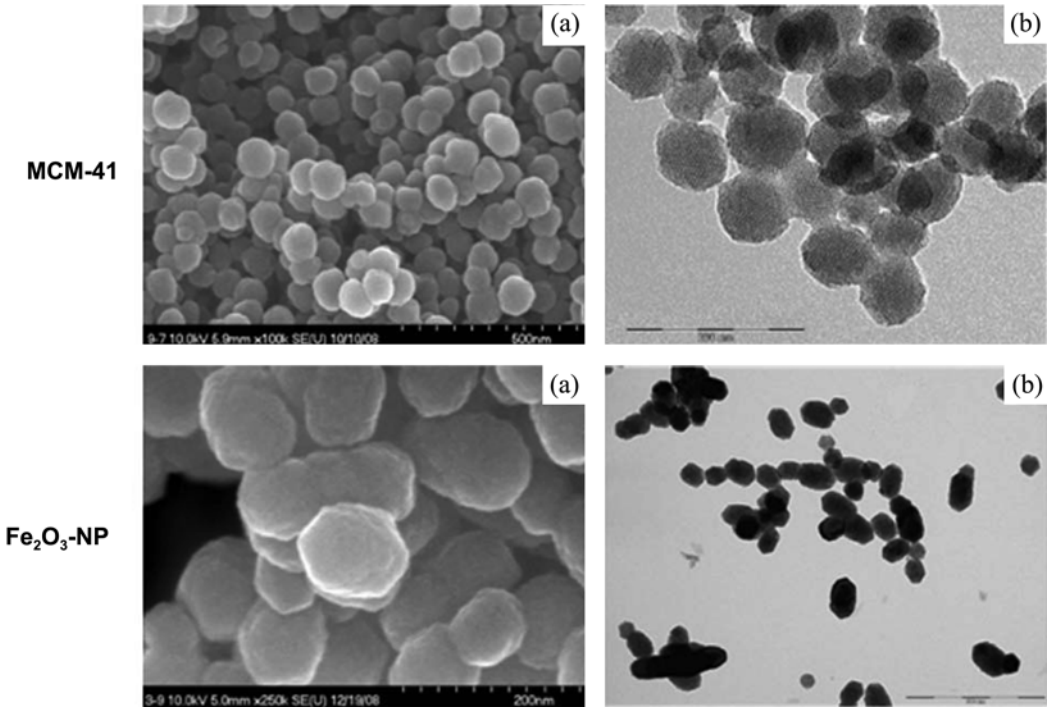

Figure S1. Scanning electron microscopic image (a) and Transmission electron microscopy image (b) of MCM-41 (up) and Fe_2O_3 nanoparticles (down).

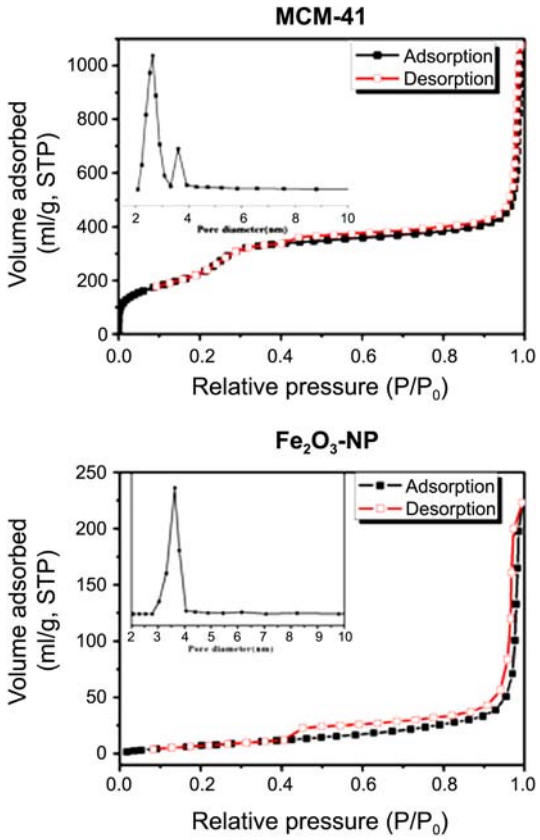

Figure S2. N2 adsorption/desorption isotherms for surface area measurement and pore size distribution (the inset) of MCM-41and Fe_2O_3 nanoparticles. Pore size distribution is given as the inset.

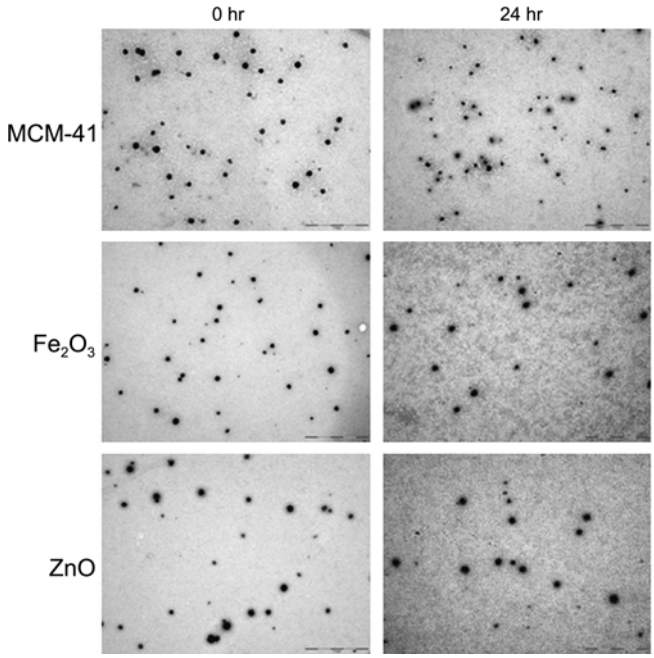

Figure S3. TEM images of nanoparticles show absence of any agglomeration in culture conditions. Test concentrations of nanparticles i.e. 100 μg/mL of MCM-41, 100 μg/mL of Fe_2O_3 and 12.5 μg/mL of ZnO were incubated for 24 h in complete medium. TEM images of NPs in culture medium with and without incubation were acquired. The scale bar measures 1 μm.

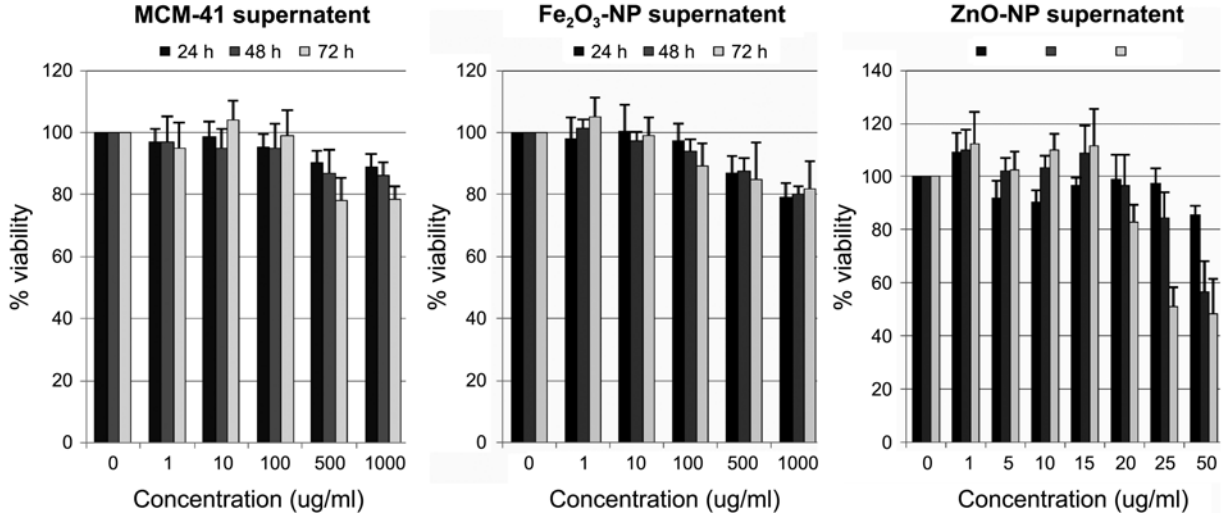

Figure S4. Cytotoxic effect of nanoparticle-associated ions released in culture medium. HEK293 cells were exposed to the NP-supernatant culture medium for the indicated time-points *viz* 24 h in presence of 24 h NP-supernatant, 48 h in presence of 48 h NP-supernatent, 72 h in presence of 72 h NP-supernatant. The toxicity was evaluated by WST-1 reagent.

Table S1. List of genes and associated biological processes altered by nanoparticles exposure
I MCM-41 regulated genes (> 2 fold)

Gene ID	Gene Name	Intensity Ratio	Enriched Gene Ontology Term
NM_001039664	tumor necrosis factor receptor superfamily, member 25	0.46	chemokine–chemokine receptor interaction
NM_001005611	ectodysplasin a	0.47	chemokine–chemokine receptor interaction
XM_370909	similar to h2a histone family, member v isoform 2	3.32	chromatin assembly-disassembly
NM_021065	histone 1, h2ad	2.44	chromatin assembly-disassembly
XM_293312	similar to h3 histone, family 3b	2.52	chromatin assembly-disassembly
NM_172220	colony stimulating factor 3 (granulocyte)	2.11	defense
NM_182707	pregnancy specific beta-1-glycoprotein 3	2.11	defense
NM_172313	colony stimulating factor 3 receptor (granulocyte)	2.16	defense
NM_014707	histone deacetylase 9	2.04	defense
NM_002784	pregnancy specific beta-1-glycoprotein 9	2.19	defense
NM_003525	histone 1, h2bd	2.35	defense
NM_153325	defensin, beta 125	2.52	defense
NM_003264	toll-like receptor 2	2.22	defense
NM_001030288	sialophorin (gpl115, leukosialin, cd43)	2.45	defense
NM_172175	interleukin 15	0.45	defense
NM_025258	chromosome 6 open reading frame 27	0.4	defense
NM_005449	fas apoptotic inhibitory molecule 3	0.45	defense
NM_138938	regenerating islet-derived 3 alpha	0.41	defense
NM_000760	colony stimulating factor 3 receptor (granulocyte)	0.4	defense
NM_152251	defensin, beta 106a	0.46	defense
NM_004977	potassium voltage-gated channel, shaw-related subfamily, member 3	0.49	gated channel activity
NM_021196	solute carrier family 4, , member 5	0.44	gated channel activity
NM_133497	potassium channel, subfamily v, member 2	0.49	gated channel activity
NM_001014797	potassium large conductance calcium-activated channel	0.47	gated channel activity
NM_000121	erythropoietin receptor	0.47	gated channel activity
NM_005628	Chemokine C-c motif ligand 8	0.44	Inflammation,
NM_000892	kallikrein b, plasma (fletcher factor) 1	0.35	Inflammation, response to wounding
NM_174872	purinergic receptor p2x,	0.45	Ion transport
NM_018979	kinase deficient protein	0.47	Ion transport
NM_001858	collagen, type xix, alpha 1	0.49	Ion transport
NM_002978	sodium channel, nonvoltage-gated 1, delta	0.44	Ion transport
NM_005416	small proline-rich protein 3	0.48	response to wounding
NM_002965	s100 calcium binding protein a9 (calgranulin b)	0.47	response to wounding
NM_001572	interferon regulatory factor 7	0.49	response to wounding
XM_496362	similar to 60s ribosomal protein l6 (tax-responsive enhancer element binding protein 107)	2.57	ribosomal processes
XM_171158	similar to ribosomal protein s2; 40s ribosomal protein s2	2.2	ribosomal processes
XM_376787	ribosomal protein s26 pseudogene 10	2.62	ribosomal processes
XM_497590	similar to 60s ribosomal protein l29 (p23)	2.34	ribosomal processes
XM_372759	similar to 60s ribosomal protein l10 (qm protein) (tumor suppressor qm) (laminin receptor homolog)	2.14	ribosomal processes
XM_928025	similar to 60s ribosomal protein l10 (qm protein) (tumor suppressor qm) (laminin receptor homolog)	3.01	ribosomal processes
XM_496363	similar to ribosomal protein s2	2.98	ribosomal processes
XM_373343	similar to 60s ribosomal protein l32	3.01	ribosomal processes
XM_927179	similar to 40s ribosomal protein s26	2.47	ribosomal processes
XM_497357	similar to ribosomal protein l10	4.7	ribosomal processes
XM_069734	similar to ribosomal protein l18	2.87	ribosomal processes
XM_060417	similar to ribosomal protein l36	2.46	ribosomal processes
XM_497657	similar to 40s ribosomal protein s16	2.3	ribosomal processes
XM_925952	similar to 40s ribosomal protein s17	2.12	ribosomal processes

II Fe_2O_3-NP regulated genes (> 2 fold)

Gene ID	Gene Name	Intensity Ratio	Enriched Gene Ontology Term
NM_005314	gastrin-releasing peptide receptor	0.35	cell proliferation
NM_004449	v-ets erythroblastosis virus e26 oncogene like (avian)	0.36	cell proliferation
NM_138279	bcl2/adenovirus e1b 19kd interacting protein like	0.42	cell proliferation
NM_002909	regenerating islet-derived 1 alpha (pancreatic stone protein)	0.42	cell proliferation
NM_002315	lim domain only 1 (rhombotin 1)	0.44	cell proliferation
NM_080718	t-box 5	0.47	cell proliferation
NM_014482	bone morphogenetic protein 10	0.48	cell proliferation
NM_033163	fibroblast growth factor 8 (androgen-induced)	0.49	cell proliferation
NM_004946	dedicator of cytokinesis 2	0.26	chemotaxis
NM_181287	cklf-like marvel transmembrane domain containing 1	0.40	chemotaxis
NM_003539	h4 histone, family 2	2.24	chromatin assembly- disassembly
NM_003513	histone 1, h2ae	2.29	chromatin assembly -disassembly
NM_003510	histone 1, h2ai	2.32	chromatin assembly -disassembly
XM_371701	similar to set protein (i-2pp2a) (taf-i) (phapii) (igaad)	2.46	chromatin assembly -disassembly
XM_370909	similar to h2a histone family, member v isoform 2	2.50	chromatin assembly -disassembly
XM_926257	similar to set protein (i-2pp2a) (taf-i)	2.54	chromatin assembly- disassembly
NM_021065	histone 1, h2ad	2.58	chromatin assembly -disassembly
NM_003493	histone 3, h3	2.71	chromatin assembly -disassembly
NM_003523,	histone 1, h2bd	2.77	chromatin assembly -disassembly
XM_293312	similar to h3 histone, family 3b	3.31	chromatin assembly -disassembly
NM_001037731	defensin, beta 116	0.48	defense
NM_058201	sperm associated antigen 11	0.49	defense
NM_002127	hla-g histocompatibility antigen, class i, g	2.02	defense
NM_002255	killer cell immunoglobulin-like receptor	2.34	defense
NM_007053	cd160 antigen	2.97	defense
NM_002173	interferon, alpha 16	0.45	defense, chemokine–chemokine receptor interaction, inflammatory response
NM_002704	pro-platelet basic protein (chemokine (c-x-c motif) ligand 7)	0.49	defense, chemokine–chemokine receptor interaction, inflammatory response, cell proliferation, chemotaxis
NM_001030288	sialophorin (gpl115, leukosialin, cd43)	2.15	defense, inflammatory response
NM_005623	chemokine (c-c motif) ligand 8	0.42	defense, response to wounding, chemokine – chemokine receptor interaction, inflammatory response, chemotaxis
NM_002965	s100 calcium binding protein a9 (calgranulin b)	0.40	defense, response to wounding, inflammatory response
NM_000491	complement component 1, q subcomponent, b chain	0.41	defense, response to wounding, inflammatory response
NM_001879	mannan-binding lectin serine peptidase 1	0.44	defense, response to wounding, inflammatory response
NM_000892	kallikrein b, plasma (fletcher factor) 1	0.44	defense, response to wounding, inflammatory response
NM_018647	TNF receptor superfamily, member 19	0.39	inflammatory response, chemokine–chemokine receptor interaction
NM_000641	interleukin 11	0.42	response to wounding, chemokine–chemokine receptor interaction, Inflammatory response, cell proliferation
NM_002001	fc fragment of IGE, receptor for alpha polypeptide	3.00	response to wounding, inflammatory response
NM_020683	adenosine a3 receptor	0.45	response to wounding, inflammatory response, defense
NM_006691	extracellular link domain containing 1	0.46	response to wounding
NM_005586	myod family inhibitor	2.01	response to wounding
NM_022161	livin inhibitor-of-apotosis	2.17	response to wounding

II Fe_2O_3-NP regulated genes (> 2 fold)

NM_002521	natriuretic peptide precursor b	0.45	renal system process
NM_001955	endothelin 1	0.49	renal system process, cell proliferation
XM_497590	similar to 60s ribosomal protein l29 (p23)	2.04	ribosomal processes
XM_294581	similar to ribosomal protein l36	2.33	ribosomal processes
XM_496991	similar to 40s ribosomal protein s26	2.47	ribosomal processes
XM_377500	similar to 40s ribosomal protein s15 (rig protein)	2.54	ribosomal processes
XM_497657	similar to 40s ribosomal protein s16	2.64	ribosomal processes
XM_496362	similar to 60s ribosomal protein l6 (taxreb107) (neoplasm-related protein c140)	2.71	ribosomal processes
XM_372759	similar to 60s ribosomal protein l10 (qm protein) (tumor suppressor qm)	2.96	ribosomal processes
XM_927179	similar to 40s ribosomal protein s26	2.98	ribosomal processes
XM_060417	similar to ribosomal protein l36	3.40	ribosomal processes
XM_925952	similar to 40s ribosomal protein s17	3.53	ribosomal processes
XM_928025	similar to 60s ribosomal protein l10 (qm protein) (tumor suppressor qm)	3.62	ribosomal processes
XM_376787	ribosomal protein s26 pseudogene 10	3.64	ribosomal processes
XM_373343	similar to 60s ribosomal protein l32	3.96	ribosomal processes
XM_496363	similar to ribosomal protein s2	4.54	ribosomal processes
XM_497357	similar to ribosomal protein l10	7.71	ribosomal processes

III ZnO-NP regulated genes (> 2 fold)

Gene ID	Gene Name	Intensity Ratio	Enriched Gene Ontology Term
NM_000204	complement factor i	0.34	activation of Immune response
NM_007360	killer cell lectin-like receptor subfamily c, member 4	0.31	activation of Immune response
NM_001001895	ubiquitin associated and sh3 domain containing, a	0.45	activation of Immune response
NM_017773	lymphocyte transmembrane adaptor 1	0.36	activation of Immune response, inactivation of MAPK
NM_021935	prokineticin 2	0.44	Ca^{2+} ion homeostasis
NM_002425	matrix metallopeptidase 10 (stromelysin 2)	8.18	Ca^{2+} ion homeostasis, inflammatory response
NM_015063	solute carrier family 8 (sodium-calcium exchanger), member 2	2.29	Ca^{2+} ion homeostasis, inflammatory response
NM_001003954	annexin a13	2.41	Ca^{2+} ion homeostasis, inflammatory response
NM_003585	double c2-like domains, beta	3.06	Ca^{2+} ion homeostasis, inflammatory response
NM_080388	s100 calcium binding protein a16	2.37	Ca^{2+} ion homeostasis, inflammatory response
NM_007087	calbindin 2, 29kda (calretinin)	2.43	Ca^{2+} ion homeostasis, inflammatory response
NM_003245	transglutaminase 3	2.07	Ca^{2+} ion homeostasis, inflammatory response
NM_002421	matrix metallopeptidase 1 (interstitial collagenase)	6.90	Ca^{2+} ion homeostasis, inflammatory response
NM_001669	arylsulfatase d	2.17	Ca^{2+} ion homeostasis, inflammatory response
NM_001039582	pregnancy upregulated non-ubiquitously expressed cam kinase	2.04	Ca^{2+} ion homeostasis, inflammatory response
NM_012076	crumbs homolog 1 (drosophila)	2.48	Ca^{2+} ion homeostasis, inflammatory response
NM_002590,	protocadherin 8	2.90	Ca^{2+} ion homeostasis, inflammatory response
NM_002770	protease, serine, 2 (trypsin 2)	2.78	Ca^{2+} ion homeostasis, inflammatory response
NM_018896	calcium channel, voltage-dependent, alpha 1g subunit	2.28	Ca^{2+} ion homeostasis, inflammatory response
NM_001734	complement component 1, s subcomponent	3.96	Ca^{2+} ion homeostasis, defense, inflammatory response, response to stress
NM_001257	cadherin 13, h-cadherin (heart)	3.99	Ca^{2+} ion homeostasis, inflammatory response, cell death
NM_002739	protein kinase c, gamma	3.41	Ca^{2+} ion homeostasis, inflammatory response, cell death, response to stress, VEGF signaling.
NM_022718	matrix metallopeptidase 25	3.11	Ca^{2+} ion homeostasis, inflammatory response, defense, response to stress
NM_000130	coagulation factor v (proaccelerin, labile factor)	2.68	Ca^{2+} ion homeostasis, inflammatory response, response to stress

III ZnO-NP regulated genes (> 2 fold)

NM_001630	annexin a8	2.38	Ca^{2+} ion homeostasis, inflammatory response, response to stress
NM_002209	integrin, alpha l (cd11a), lymphocyte function-associated antigen 1)	2.88	Ca^{2+} ion homeostasis, inflammatory response, T cell activation,
NM_032562	phospholipase a2, group xiib	4.76	Ca^{2+} ion homeostasis, inflammatory response, VEGF signaling
NM_000300	phospholipase a2, group iia (platelets, synovial fluid)	6.54	Ca^{2+} ion homeostasis, inflammatory response, VEGF signaling
NM_004166	chemokine (c-c motif) ligand 14	0.45	Ca^{2+} ion homeostasis, metal ion homeostasis, chemokine–chemokine receptor interaction
NM_002985	chemokine (c-c motif) ligand 5	0.49	Ca^{2+} ion homeostasis, metal ion homeostasis, response to oxidative stress, chemotaxis
NM_002062	glucagon-like peptide 1 receptor	0.43	Ca^{2+} ion homeostasis, metal ion homeostasis
NM_000576	interleukin 1, beta	0.36	Ca^{2+} ion homeostasis, metal ion homeostasis
NM_002575	serpin peptidase inhibitor, clade b	2.03	cell death
NM_004131	granzyme b (granzyme 2)	2.70	cell death
NM_021972	sphingosine kinase 1	2.73	cell death
NM_182985	ring finger protein 36	2.53	cell death
NM_000125	estrogen receptor 1	2.05	cell death
NM_004115	fibroblast growth factor 14	2.07	cell death
NM_004049	bcl2-related protein a1	2.97	cell death
NM_002457	mucin 2, intestinal/tracheal	5.83	cell death
NM_033183	chorionic gonadotropin, beta polypeptide	2.04	cell death
NM_000061	bruton agammaglobulinemia tyrosine kinase	2.69	cell death
NM_022740	homeodomain interacting protein kinase 2	2.15	cell death
NM_001885	crystallin, alpha b	3.00	cell death
NM_005627	serum/glucocorticoid regulated kinase	2.05	cell death, response to stress
NM_015675	growth arrest and dna-damage-inducible, beta	3.40	cell death, response to stress
NM_002133	heme oxygenase (decy	2.72	cell death, response to stress
NM_006705	growth arrest and dna-damage-inducible,	2.52	cell death, response to stress
NM_000948	prolactin	0.83	chemokine –chemokine receptor interaction
NM_148968	TNF receptor superfamily, member 25	0.42	chemokine –chemokine receptor interaction
NM_000163	growth hormone receptor	0.49	chemokine –chemokine receptor interaction
NM_000206	interleukin 2 receptor, gamma	0.47	chemokine –chemokine receptor interaction
NM_000799	erythropoietin	0.48	chemokine –chemokine receptor interaction
NM_002173	interferon, alpha 16	0.44	chemokine –chemokine receptor interaction
NM_000595	lymphotoxin alpha (TNF superfamily, member 1)	5.11	chemokine –chemokine receptor interaction, cell death
NM_001039664	TNF receptor superfamily, member 25	3.03	chemokine –chemokine receptor interaction, cell death
NM_001243	TNF receptor superfamily, member 8	2.56	chemokine –chemokine receptor interaction, cell death
NM_006850	interleukin 24	2.47	chemokine –chemokine receptor interaction, cell death, Jak-Stat signaling
NM_013246	cardiotrophin-like cytokine factor 1	2.84	chemokine –chemokine receptor interaction, cell death, Jak-Stat signaling
NM_004887	chemokine (c-x-c motif) ligand 14	0.45	chemokine –chemokine receptor interaction, chemotaxis
NM_001842	ciliary neurotrophic factor receptor	2.17	chemokine –chemokine receptor interaction, Jak-Stat signaling
NM_000760	colony stimulating factor 3 receptor (granulocyte)	2.02	chemokine –chemokine receptor interaction, Jak-Stat signaling
NM_175725	interleukin 5 receptor, alpha	2.52	chemokine –chemokine receptor interaction, Jak-Stat signaling
NM_002185	interleukin 7 receptor	2.33	chemokine –chemokine receptor interaction, Jak-Stat signaling
NM_172247	colony stimulating factor 2 receptor, alpha	2.06	chemokine –chemokine receptor interaction, Jak-Stat signaling
NM_001012288	cytokine receptor-like factor 2	2.29	chemokine –chemokine receptor interaction, Jak-Stat signaling

III ZnO-NP regulated genes (> 2 fold)

NM_000641	interleukin 11	2.11	response to stress, chemokine –chemokine receptor interaction, Jak-Stat signaling,
NM_005118	TNF (ligand) superfamily, member 15	0.37	chemokine –chemokine receptor interaction, negative regulator of cell proliferation
NM_020530	oncostatin m	2.17	cell death, chemokine–chemokine receptor interaction, response to stress, Jak-Stat signaling,
NM_000185	serpin peptidase inhibitor, clade d, member 1	0.43	chemotaxis
NM_181283	cklf-like marvel transmembrane domain containing 1	0.46	chemotaxis
NM_002780	pregnancy specific beta-1-glycoprotein 4	2.03	defense
NM_138720	histone 1, h2bd	2.09	defense
NM_014391	ankyrin repeat domain 1 (cardiac muscle)	2.35	defense
NM_080593	histone 1, h2bk	2.15	defense
NM_000265	neutrophil cytosolic factor 1,	2.03	defense
NM_005546	il2-inducible t-cell kinase	3.01	defense
NM_182707	pregnancy specific beta-1-glycoprotein 3	3.06	defense
NM_005438	fos-like antigen 1	2.69	defense
NM_006433	granulysin	2.32	defense
NM_001033019	beta-defensin 134	2.17	defense
NM_000433	neutrophil cytosolic factor 2	3.41	defense
NM_002784	pregnancy specific beta-1-glycoprotein 9	2.86	defense
NM_001005176	sp140 nuclear body protein	2.11	defense
NM_033004	nacht, leucine rich repeat and pyd containing 1	2.17	defense, cell death
NM_005449	fas apoptotic inhibitory molecule 3	2.50	defense, cell death
NM_003706	phospholipase a2, group ivc	2.28	defense, cell death, inflammatory response
NM_002192	inhibin, beta a (activin a, activin ab alpha polypeptide)	4.83	defense, chemokine –chemokine receptor interaction, cell death
NM_000594	tumor necrosis factor (tnf superfamily, member 2)	2.50	defense, chemokine –chemokine receptor interaction, cell death
NM_017417	n-acetylgalactosaminyltransferase 8 (galnac-t8)	2.58	defense, inflammatory response
NM_017581	cholinergic receptor, nicotinic, alpha 9	2.43	defense, inflammatory response
NM_020359	phospholipid scramblase 2	2.24	defense, inflammatory response
NM_003241	transglutaminase 4 (prostate)	2.72	defense, inflammatory response
NM_005965	myosin, light polypeptide kinase	2.39	defense, inflammatory response
NM_004994	matrix metallopeptidase 9 (gelatinase b)	2.15	defense, inflammatory response, cell death
NM_000064	complement component 3	2.13	defense, inflammatory response, response to stress
NM_000063	complement component 2	2.49	defense, inflammatory response, response to stress
NM_023068	sialic acid binding ig-like lectin 1, sialoadhesin	2.37	defense, inflammatory response, response to stress
NM_001033952	calcitonin/calcitonin-related polypeptide, alpha	2.10	defense, inflammatory response, response to stress
NM_005252	v-fos fbj murine osteosarcoma viral oncogene homolog	13.73	defense, inflammatory response, response to stress
NM_004433	e74-like factor 3	2.20	defense, inflammatory response, response to stress
NM_001063	transferrin	6.58	defense, inflammatory response, response to stress
NM_001337	chemokine (c-x3-c motif) receptor 1	2.27	defense, inflammatory response, response to stress
NM_052872	interleukin 17f	6.91	defense, inflammatory response, response to stress
NM_148888	chemokine (c-c motif) ligand 25	3.81	defense, inflammatory response, response to stress, chemokine–chemokine receptor interaction
NM_006137	cd7 antigen (p41)	2.45	defense, T cell activation
NM_002286	lymphocyte-activation gene 3	2.12	defense, T cell activation , cell death
NM_080876	dual specificity phosphatase 19	0.47	inactivation of MAPK
NM_002716	protein phosphatase 2, regulatory subunit a isoform	0.47	inactivation of MAPK
NM_003407	zinc finger protein 36, c3h type, homolog (mouse)	3.20	Inflammatory response, response to stress
NM_000901	nuclear receptor subfamily 3, groupc, member 2	0.47	metal ion homeostasis
NM_004923	metallothionein-like 5, testis-specific (tesmin)	0.43	metal ion homeostasis, response to oxidative stress
NM_005953	metallothionein 2a	10.31	metallothionein superfamily
NM_005951	metallothionein 1h	21.41	metallothionein superfamily

III ZnO-NP regulated genes (> 2 fold)

NM_005952	metallothionein 1x	14.36	metallothionein superfamily
NM_005950	metallothionein 1g	36.32	metallothionein superfamily
NM_005947	metallothionein 1b (functional)	16.53	metallothionein superfamily
NM_005949	metallothionein 1f (functional)	28.56	metallothionein superfamily
NM_080757	chromosome 20 open reading frame 127	2.93	metallothionein superfamily
NM_175622	metallothionein 1j (pseudogene)	15.92	metallothionein superfamily
NM_178543	ectonucleotide pyrophosphatase 7	0.36	negative regulation of cell proliferation
NM_000914	opioid receptor, mu 1	0.46	negative regulation of cell proliferation
NM_003641	interferon induced transmembrane protein 1 (9-27)	0.49	negative regulation of cell proliferation
NM_000551	von hippel-lindau tumor suppressor	0.37	negative regulation of cell proliferation
NM_003225	trefoil factor 1	0.44	negative regulation of cell proliferation
NM_001050	somatostatin receptor 2	0.40	negative regulation of cell proliferation
NM_021146	angiopoietin-like 7	0.45	response to oxidative stress
NM_000502	eosinophil peroxidase	0.45	response to oxidative stress
NM_000636	superoxide dismutase 2, mitochondrial	0.18	response to oxidative stress
NM_000602	serpin peptidase inhibitor, clade e	2.96	response to stress
NM_001012964	kallikrein 6	4.19	response to stress
NM_002155	heat shock 70kda protein 6	66.61	response to stress
NM_015831	acetylcholinesterase	2.89	response to stress
NM_000020	activin a receptor type ii-like 1	2.68	response to stress
NM_006308	heat shock 27kda protein 3	5.40	response to stress
NM_012323	v-maf musculoaponeurotic fibrosarcoma oncogene homolog f	4.45	response to stress
NM_000798	dopamine receptor d5	2.37	response to stress
NM_000088	collagen, type i, alpha 1	2.09	response to stress
NM_000353	tyrosine aminotransferase	2.23	response to stress
NM_004931	cd8 antigen, beta polypeptide 1 (p37)	2.02	T cell activation
NM_001964	early growth response 1	5.04	T cell activation
NM_014143	cd274 antigen	3.00	T cell activation
NM_000193	sonic hedgehog homolog (drosophila)	3.47	T cell activation
NM_012411	protein tyrosine phosphatase, non-receptor type 22	3.12	T cell activation
NM_005356	lymphocyte-specific protein tyrosine kinase	4.13	T cell activation, cell death
NM_001025158	cd74 antigen	3.39	T cell activation, cell death
NM_021972	sphingosine kinase 1	2.73	VEGF signaling
NM_002872	rho family, small gtp binding protein rac2	2.42	VEGF signaling
NM_003975	sh2 domain protein 2a	2.18	VEGF signaling

Table S2. Sequence of Primer pairs used in the study

Genes	Forward Primer (5'-3')	Reverse Primer (3'-5')
Metallothionein 2a (MT2a)	ACTTGGCACAGCCCACAG	GACTCTAGCCGCCTCTTCAG
v-fos fbj murine osteosarcoma viral oncogene homolog	CCGGGGATAGCCTCTCTTAC	AGGTCCGGACTGGTCGAG
Interleukin17f (IL17f)	TGGCATCATCAATGAAAACC	TTCCTTGAGCATTGATGCAG
Chemokine cc motif ligand 15 (CCL15)	GCTTGTTGCTGTCCTTGGAT	GAGTGAACACGGGATGCTTT
Heat shock 70kDa protein 6 (HSPA6)	GAGATCTCGTCCATGGTGCT	TTGATGATCCGCAACACG
Matrix metallopeptidase 1 (MMP1)	TGGCATCATCAATGAAAACC	TTCCTTGAGCATTGATGCAG
Pregnancy specific beta-1-glycoprotein 8 (PSG1)	GACGCAGGATCCTACACCTT	GGTTAAGCTCACAGCCTCCA
Pregnancy specific beta-1-glycoprotein (PSG9)	AGCTGCCCATCCCCTACAT	GGCTCTGACCGTTTAGCCA